U.S. ARMY COMBAT CAPABILITIES DEVELOPMENT COMMAND – ARMAMENTS CENTER

STEEL FI BARRIERS HARDNESS AND OBLIQUITY EFFECTS

Kevin T. Miers, Daniel L. Prillaman, Eric A. Lynd, Nausheen M. Al-Shehab

2022 Insensitive Munitions and Energetic Materials Technology Symposium

Indianapolis, IN, USA

Presented by Kevin T. Miers, Mechanical Engineer

US Army DEVCOM AC Detonation Physics and Experimental Research Branch

Phone: 973-724-1180 Email: kevin.t.miers.civ@army.mil

UNCLASSIFIED

OVERVIEW

- NATO IM Fragment Impact (FI) testing
- Penetration mechanics considerations
- High hardness armor steels
- Experimental methodology
- Test Results
- Discussion and preliminary hydrocode models
- Summary and conclusions

NATO IM FRAGMENT IMPACT TESTING

- NATO standard FI test (STANAG 4496) [1]
  - 14.3mm diameter, 18.6g, L/D~1, 160° conical nosed fragment
  - Mild steel, Brinell hardness <270
    - **New requirement: BHN > 190**
  - 2530±90 m/s impact velocity
  - Aimpoints: center of largest presented area of HE or most shock sensitive location
- Smooth bore 40mm powder gun often used in the U.S. [2]
  - Commercially available, used by various test facilities
  - Powder charge adjusted to obtain correct velocity
  - Replaceable wear section
  - Plastic sabot machined to fit

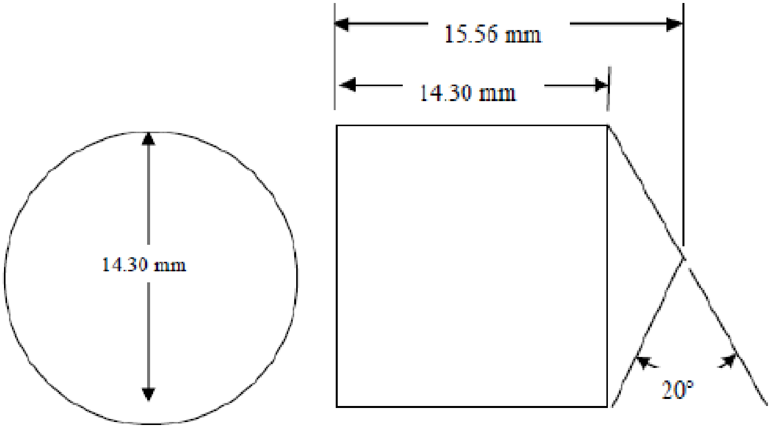

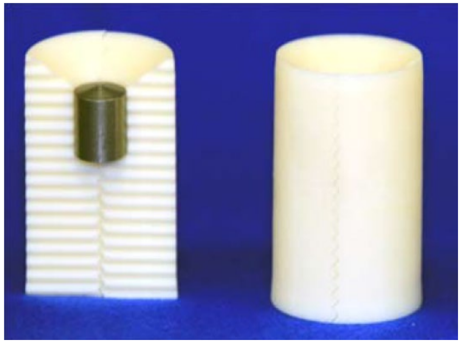

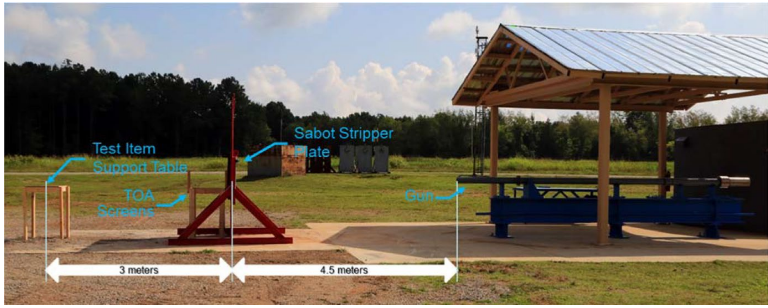

NATO IM FRAGMENT IMPACT TESTING (CONT'D)

Steel	Treatment	Yield stress MPa	Yield stress ksi	Tensile stress MPa	Tensile stress ksi	Elongation, %
1020	Normalized	345	50	440	64	36
1040	(air cooled)	370	54	595	86	28
1095		505	73	1015	147	9.5
1020	As rolled	330	48	450	65	35
1040		415	60	620	90	25
1095		570	83	965	140	9

1018 commonly used

(from [3])

HRC	HV	HB(a)	HRA	HRB	Ultimate tensile strength MPa	Ultimate tensile strength ksi
29	294	279	64.7	(104.5)	931	135
28	286	271	64.3	(104.0)	910	132
27	279	264	63.8	(103.0)	883	128
(14)	213	203	...	93.9	676	98
(12)	204	194	...	92.3	648	94
(10)	196	187	...	90.7	621	90

~BHN 270

~BHN 190

Probably need to use higher carbon content steel (>1040)

PENETRATION MECHANICS HARDNESS EFFECTS

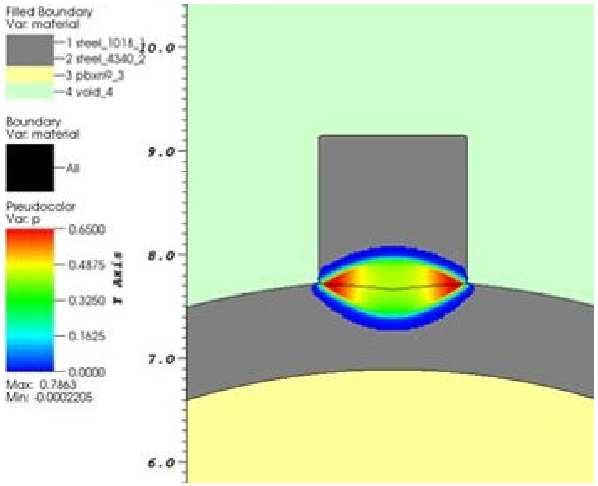

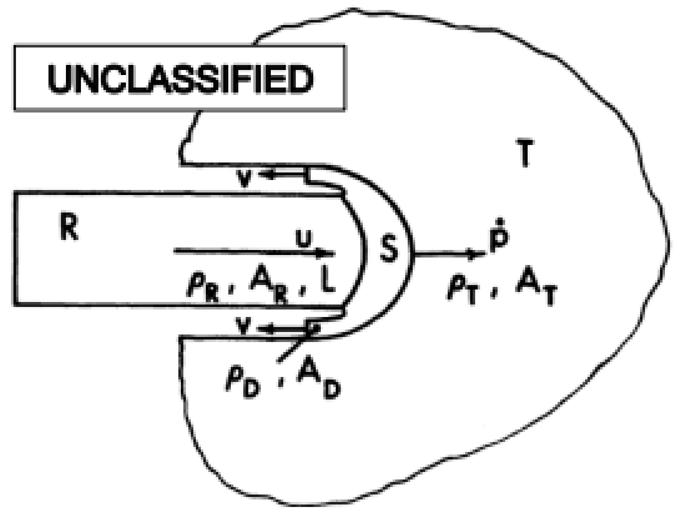

Note: from BRL-TR-2759.

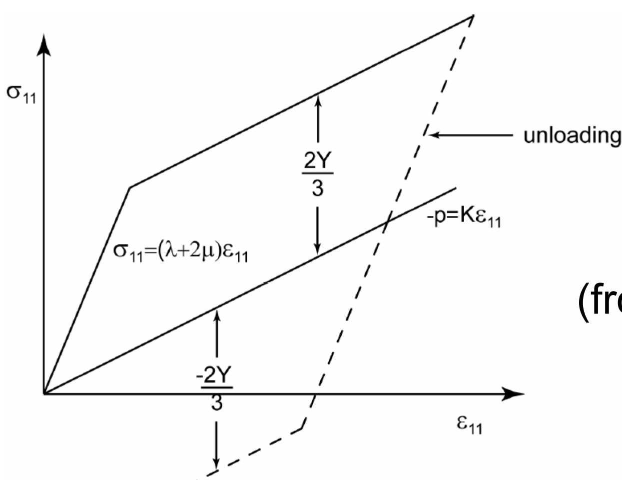

(from [6])

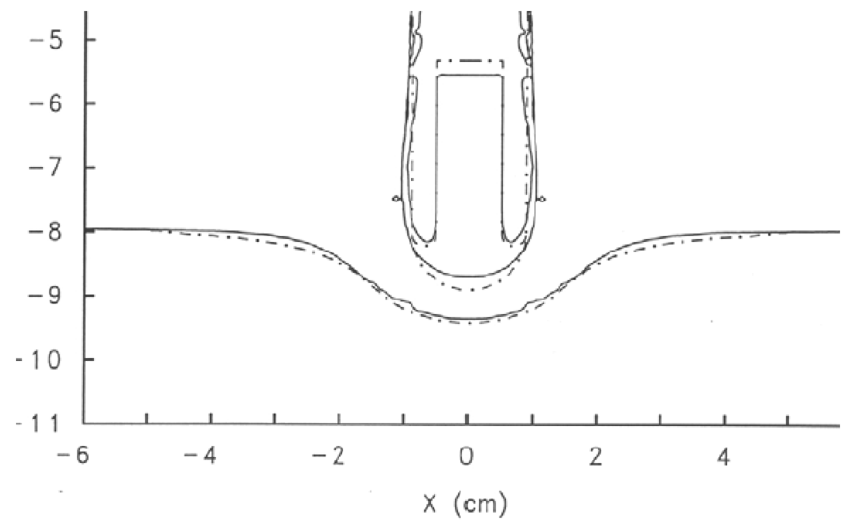

PENETRATION MECHANICS FAILURE EFFECTS

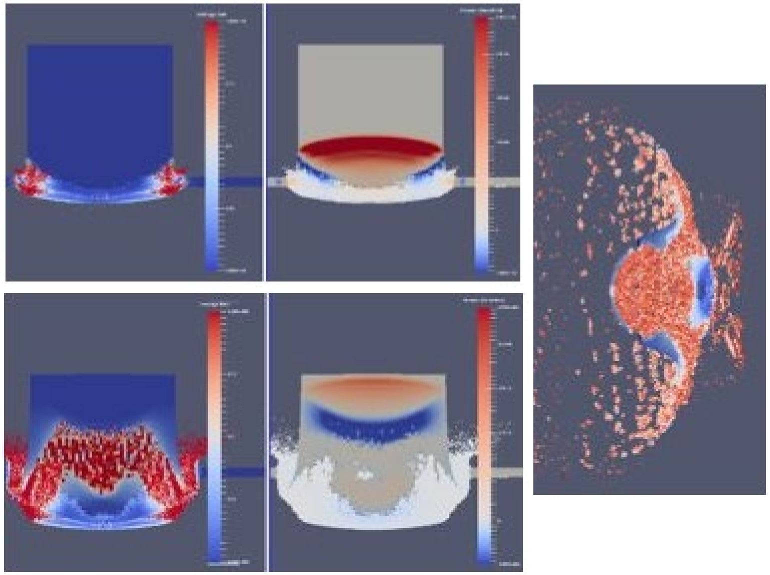

$$P_s = (3\rho_0 c_0 K_c^2 \dot{\varepsilon})^{\frac{1}{3}}$$

Brittle spall strength [4]

$$P_s = (2\rho_0 c_0^2 Y \varepsilon_f)^{\frac{1}{2}}$$

Ductile spall strength [4]

$$s = 2c_K t = 2c_K \frac{\varepsilon}{\dot{\varepsilon}} = \sqrt{\frac{8Y\varepsilon_f}{\rho}}\ \frac{1}{\dot{\varepsilon}}$$

Grady ductile fragmentation [6]

$$s = \left(\frac{\sqrt{24}K_c}{\rho\, c_K\, \dot{\varepsilon}}\right)^{2/3}$$

Grady brittle fragmentation [6]

$$x_0 = (2P_F/\rho\gamma)^{\frac{1}{2}}\, r/v.$$

Mott fragmentation [12]

$$N(m) = \frac{M_0}{2M_K^2}\, e^{-\left(\frac{m^{1/2}}{M_K}\right)}$$

Mott distribution [12]

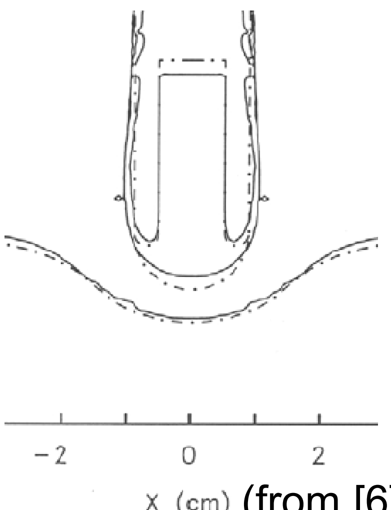

(from [6])

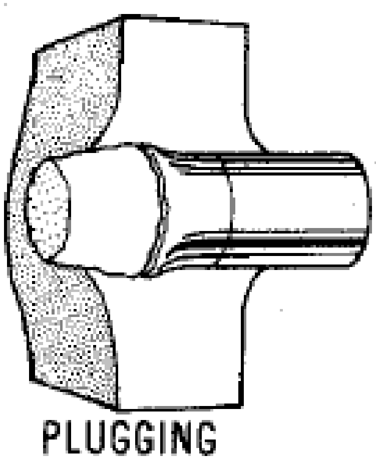

STEEL ARMOR TECHNOLOGY

- Hardness vs. toughness, ductility
  - Ancillary requirements: cost, structural integrity, manufacturing considerations, multi-hit, environmental
- Heat treatment (quenching and tempering)
- Cast armor
- Rolled homogeneous armor
- Face hardened armor
- High hardness armor
- Ultra high hardness armor
- Metal laminated composites (Dual Hardness)
- Improved metallurgical processing for cast ingots: unidirectional casting, electroslag remelting (ESR)
- Dual hardness ESR

STEEL ARMOR TECHNOLOGY

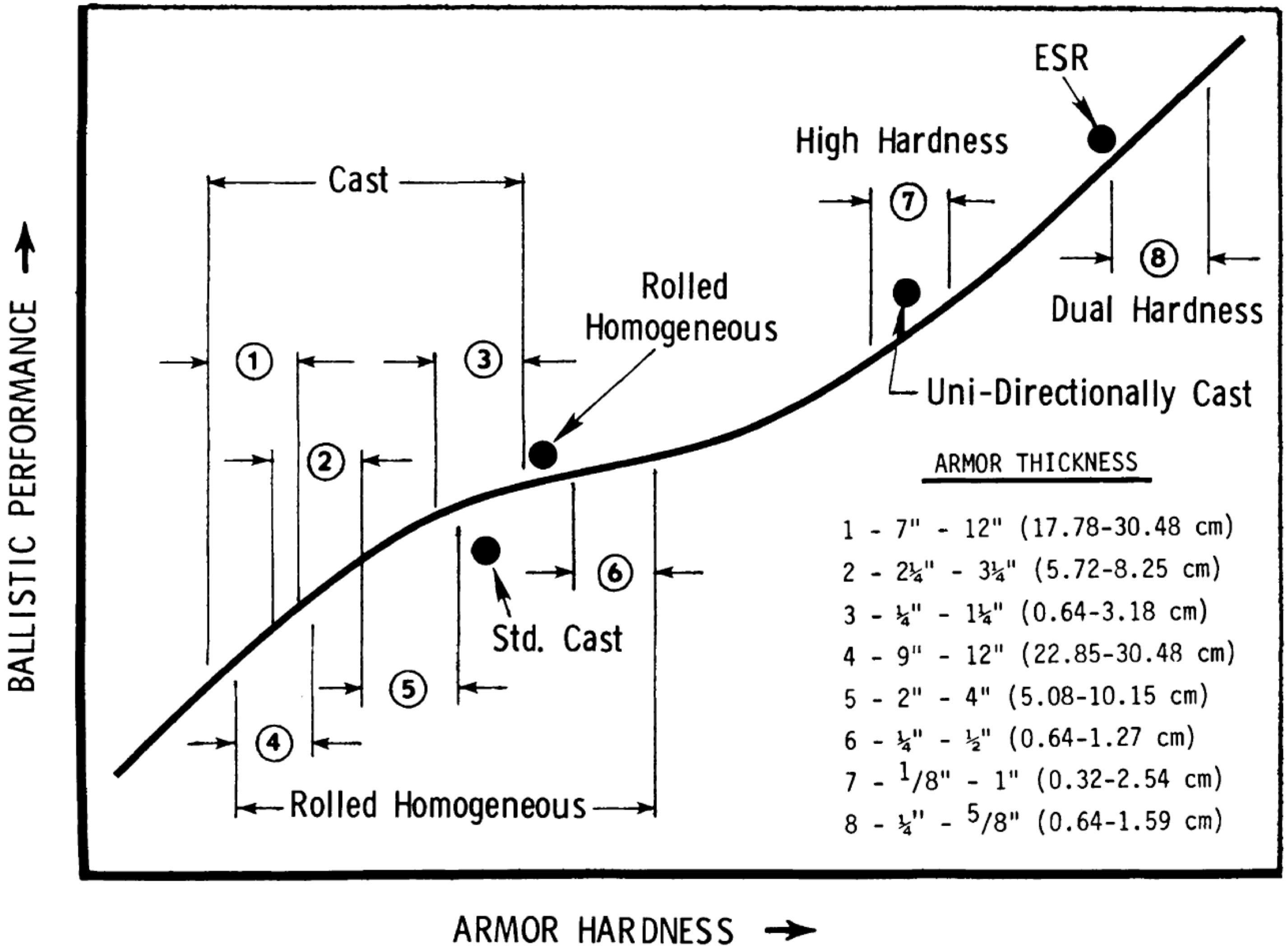

EXPERIMENTAL METHODOLOGY

Table 3: Test Matrix

Test No.	Thickness (in)	Material	Obliquity (deg)
RT21-469	0.125	4340 RC38	0
RT21-470	0.250	4340 RC38	0
RT21-471	0.088	4340 RC38	45
RT21-472	0.177	4340 RC38	45
RT21-473	0.125	D2 Tool Steel RC60	0
RT21-474	0.250	D2 Tool Steel RC60	0
RT21-475	0.088	D2 Tool Steel RC60	45
RT21-478	0.177	D2 Tool Steel RC60	45

TEST SETUP

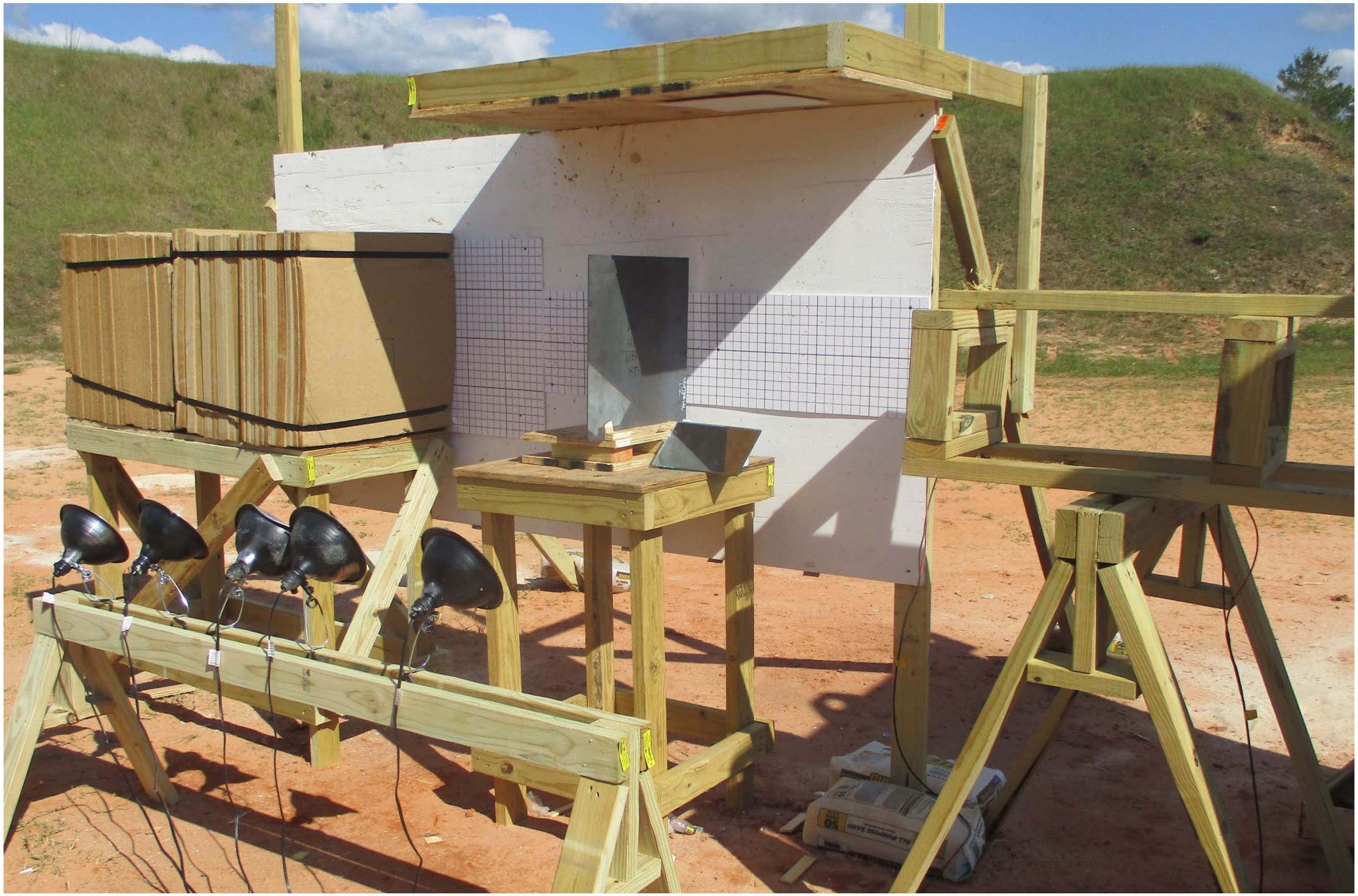

RT469, 0.125”, 4340 RC38, 0 DEG OBLIQUITY

Fig. C1. RT21-469 (0.125”, 4340 RC38, 0° Obliquity) high speed video frames at -100us, 0us, 50us, 100us, 150us, 200us, 300us

RT469, 0.125", 4340 RC38, 0 DEG OBLIQUITY

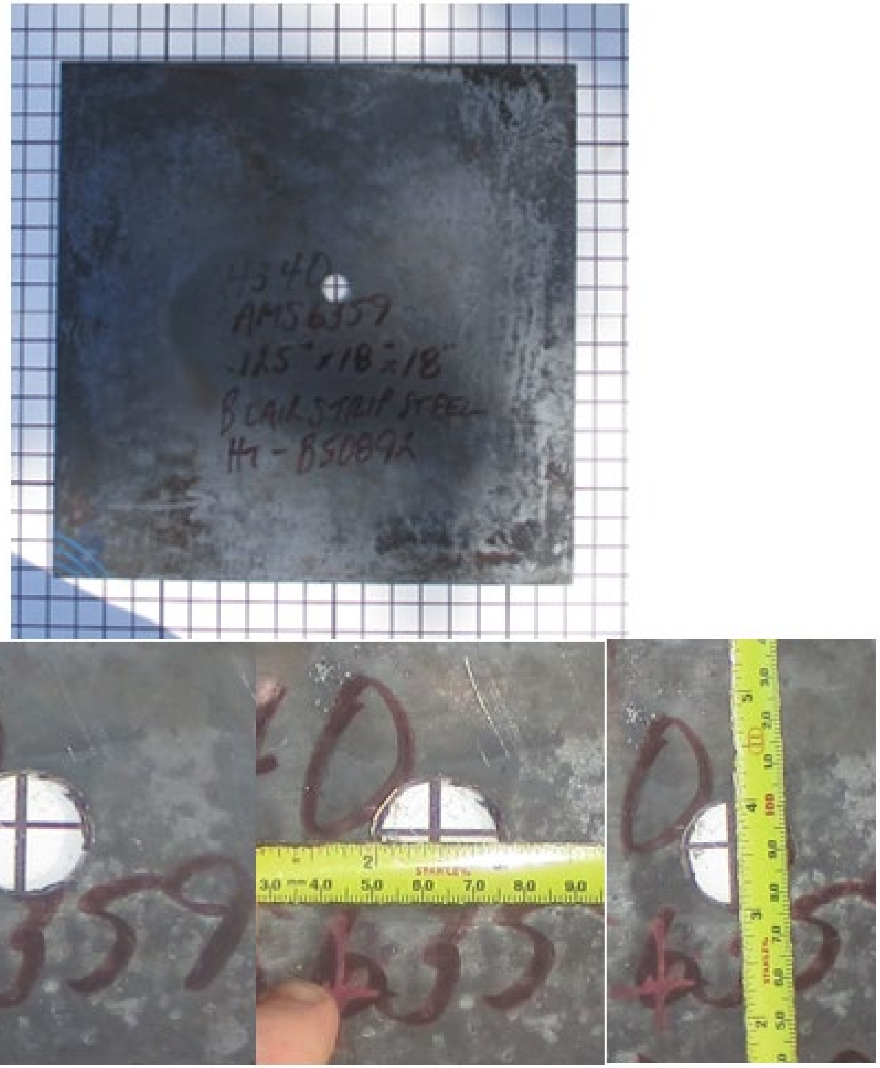

Fig. D1. RT21-469: 4340 RC38 Steel 0.125" Thick, 0 Degrees Obliquity

RT470, 0.250”, 4340 RC38, 0 DEG OBLIQUITY

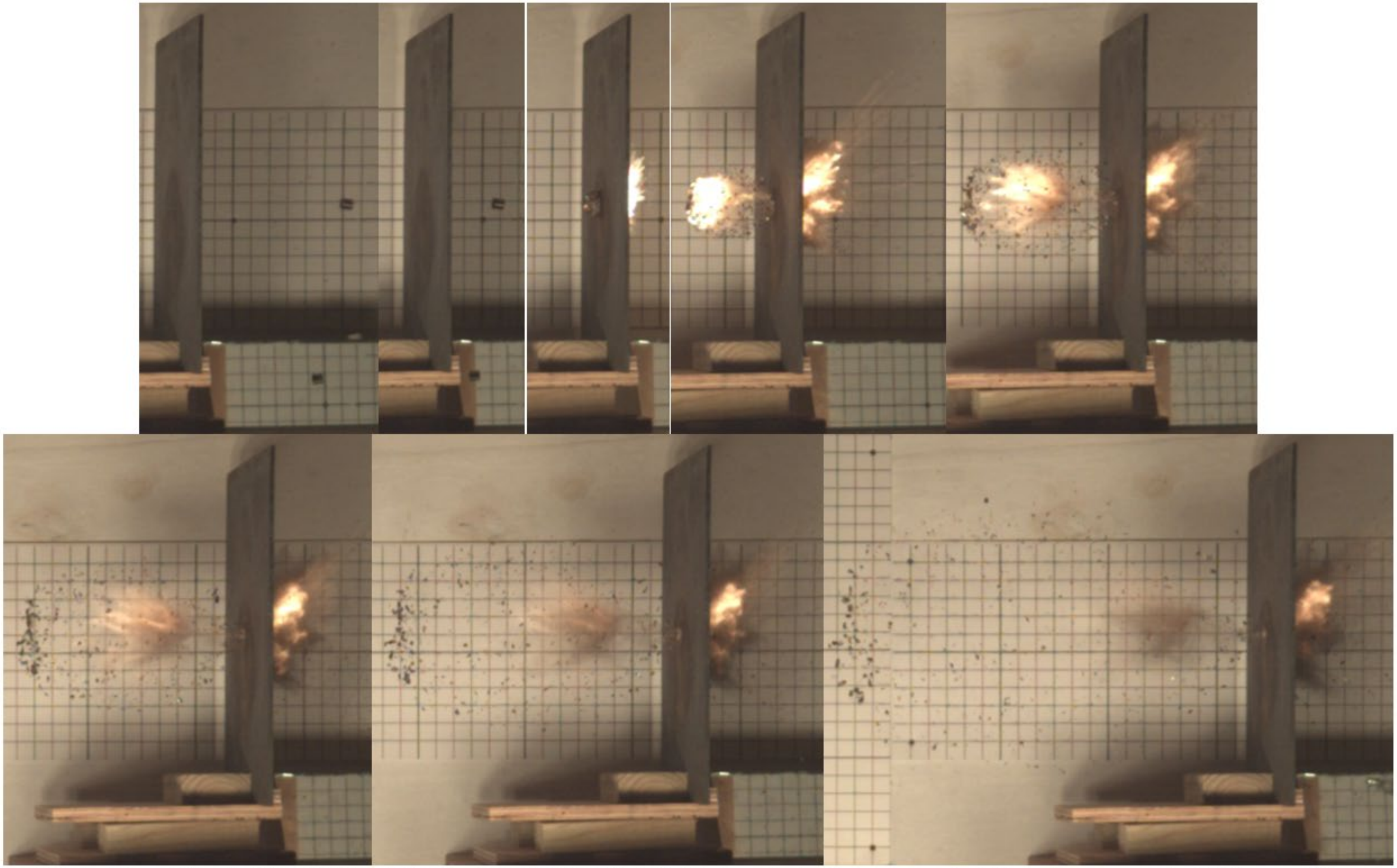

Fig. C2. RT21-470 (0.250”, 4340 RC38, 0° Obliquity) high speed video frames at -100us, -50us, 0us, 50us, 100us, 150us, 200us, 300us

RT470, 0.250”, 4340 RC38, 0 DEG OBLIQUITY

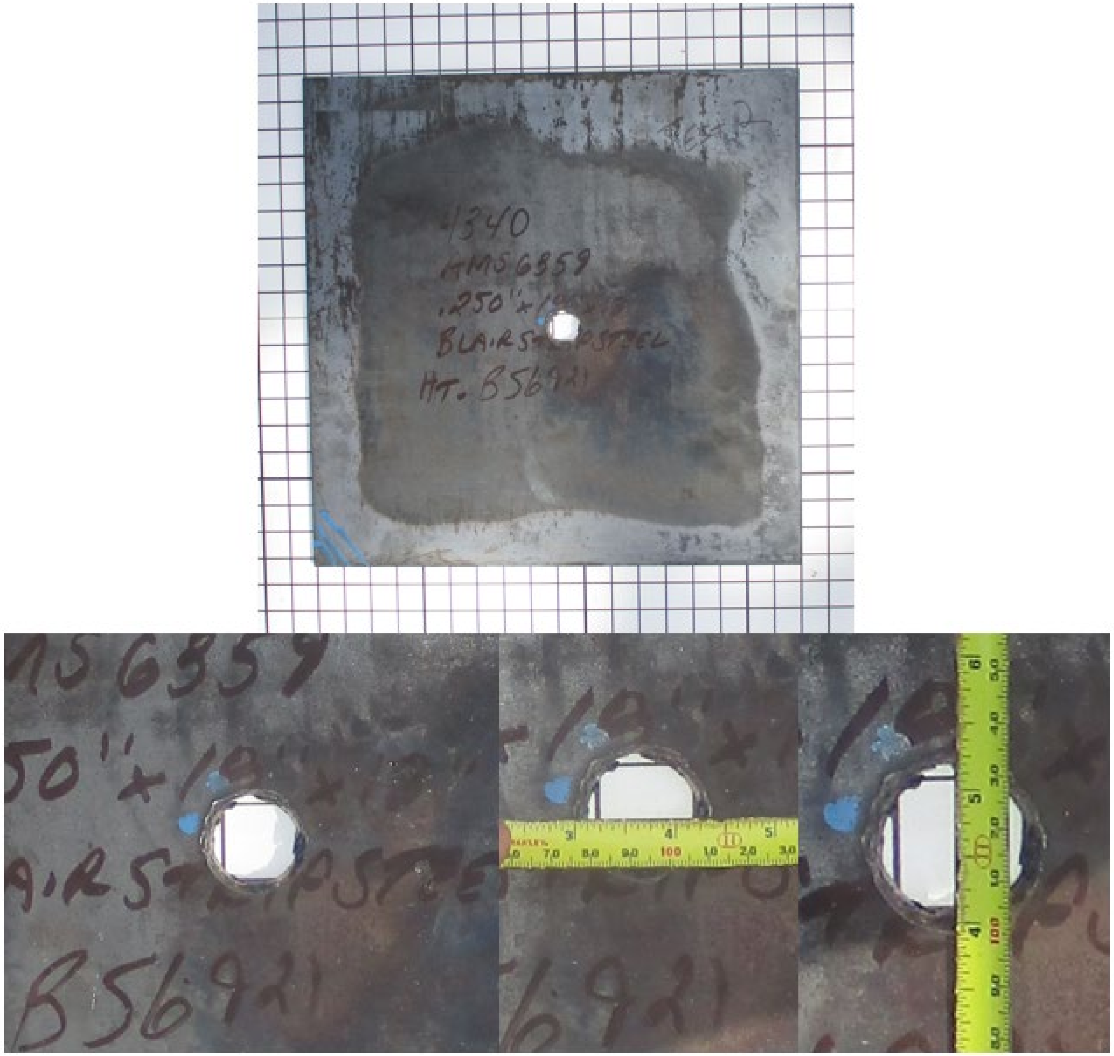

Fig. D2. RT21-470: 4340 RC38 Steel 0.25” Thick, 0 Degrees Obliquity

RT471, 0.088”, 4340 RC38, 45 DEG OBLIQUITY

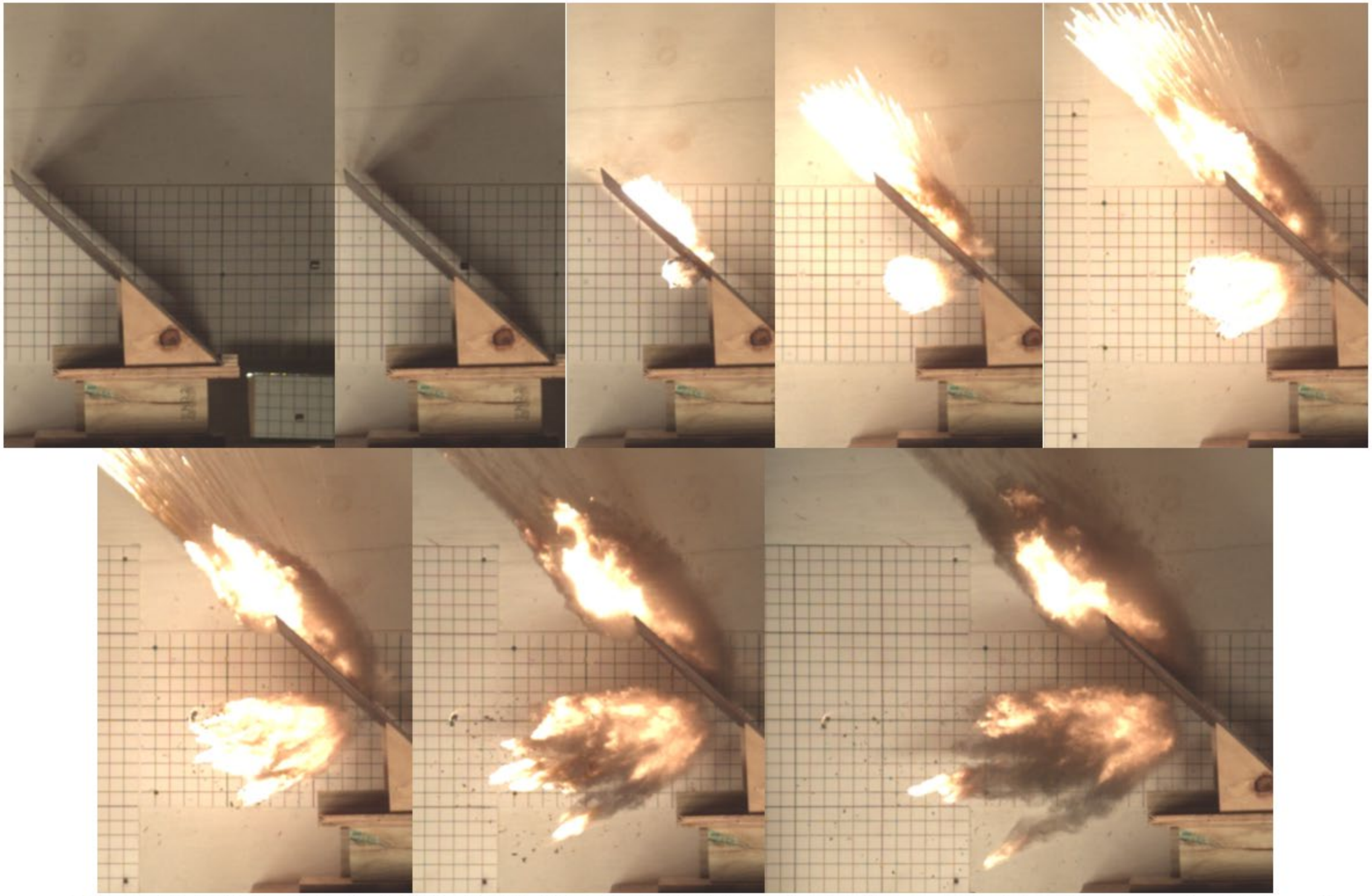

Fig. C3. RT21-471 (0.088”, 4340 RC38, 45° Obliquity) high speed video frames at -120us, 0us, 40us, 80us, 120us, 160us, 240us, 320us

RT471, 0.088”, 4340 RC38, 45 DEG OBLIQUITY

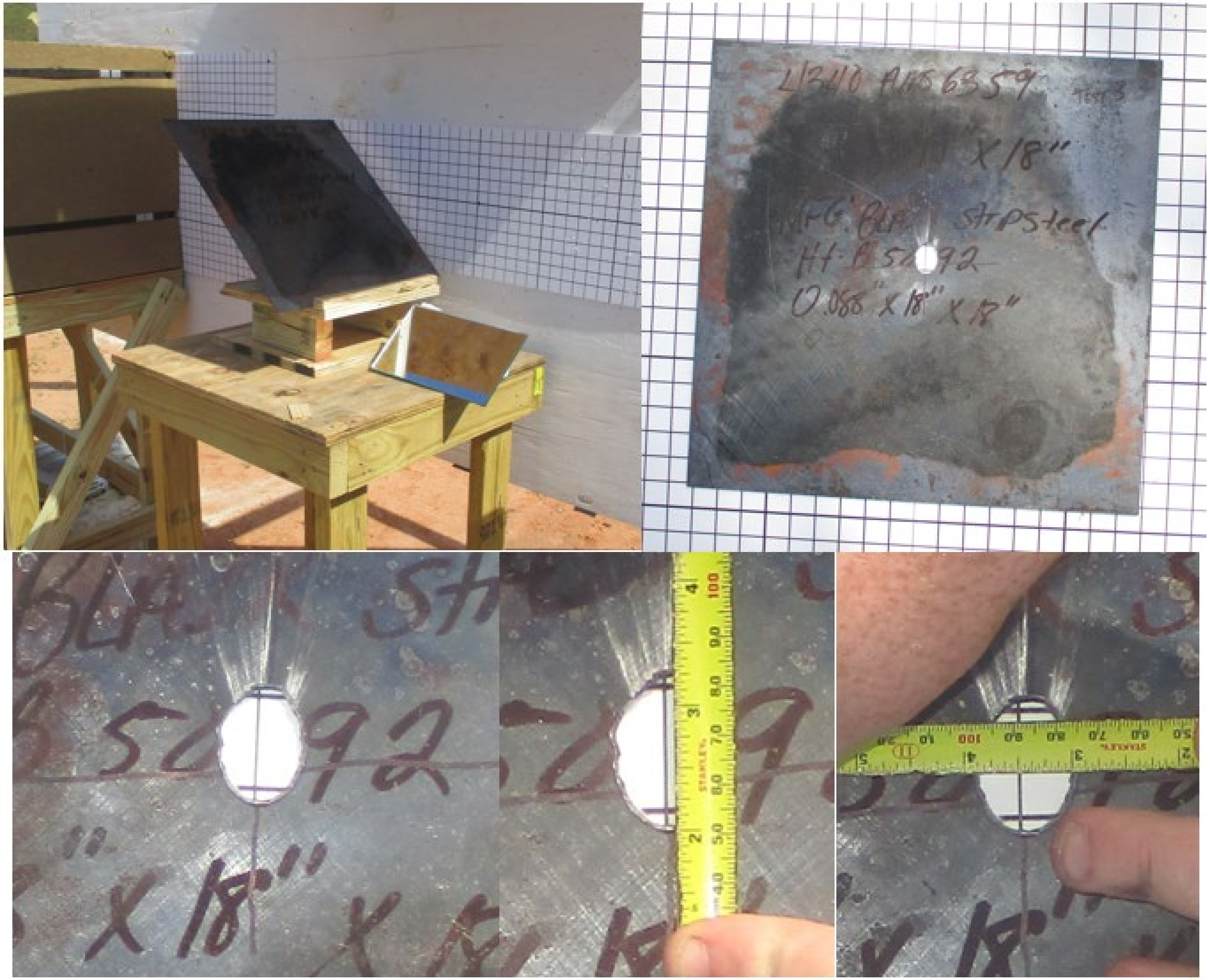

Fig. D3. RT21-471: 4340 RC38 Steel 0.088” Thick, 45 Degrees Obliquity

RT472, 0.177”, 4340 RC38, 45 DEG OBLIQUITY

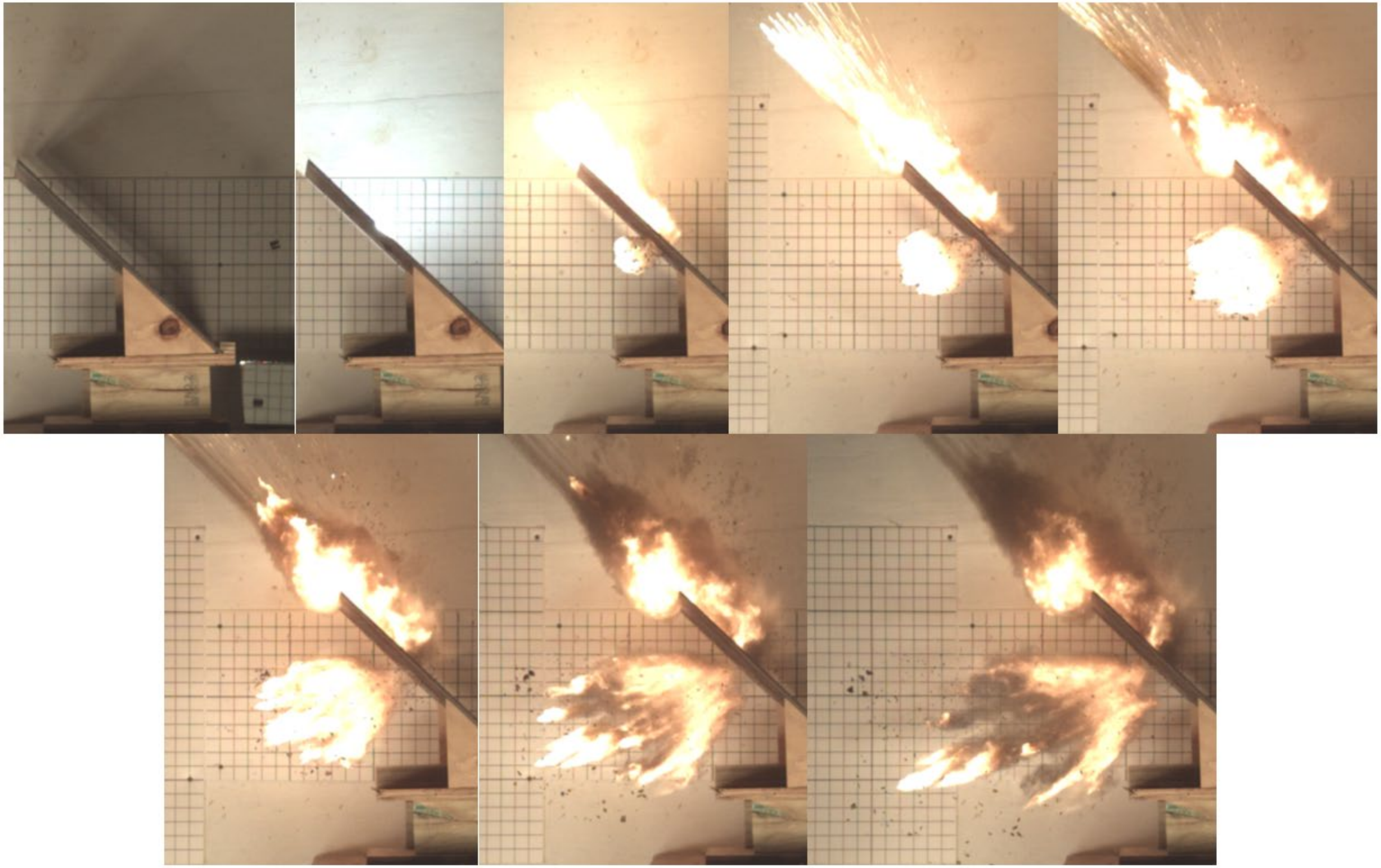

Fig. C4. RT21-472 (0.177”, 4340 RC38, 45° Obliquity) high speed video frames at -120us, 0us, 40us, 80us, 120us, 160us, 240us, 320us

RT472, 0.177”, 4340 RC38, 45 DEG OBLIQUITY

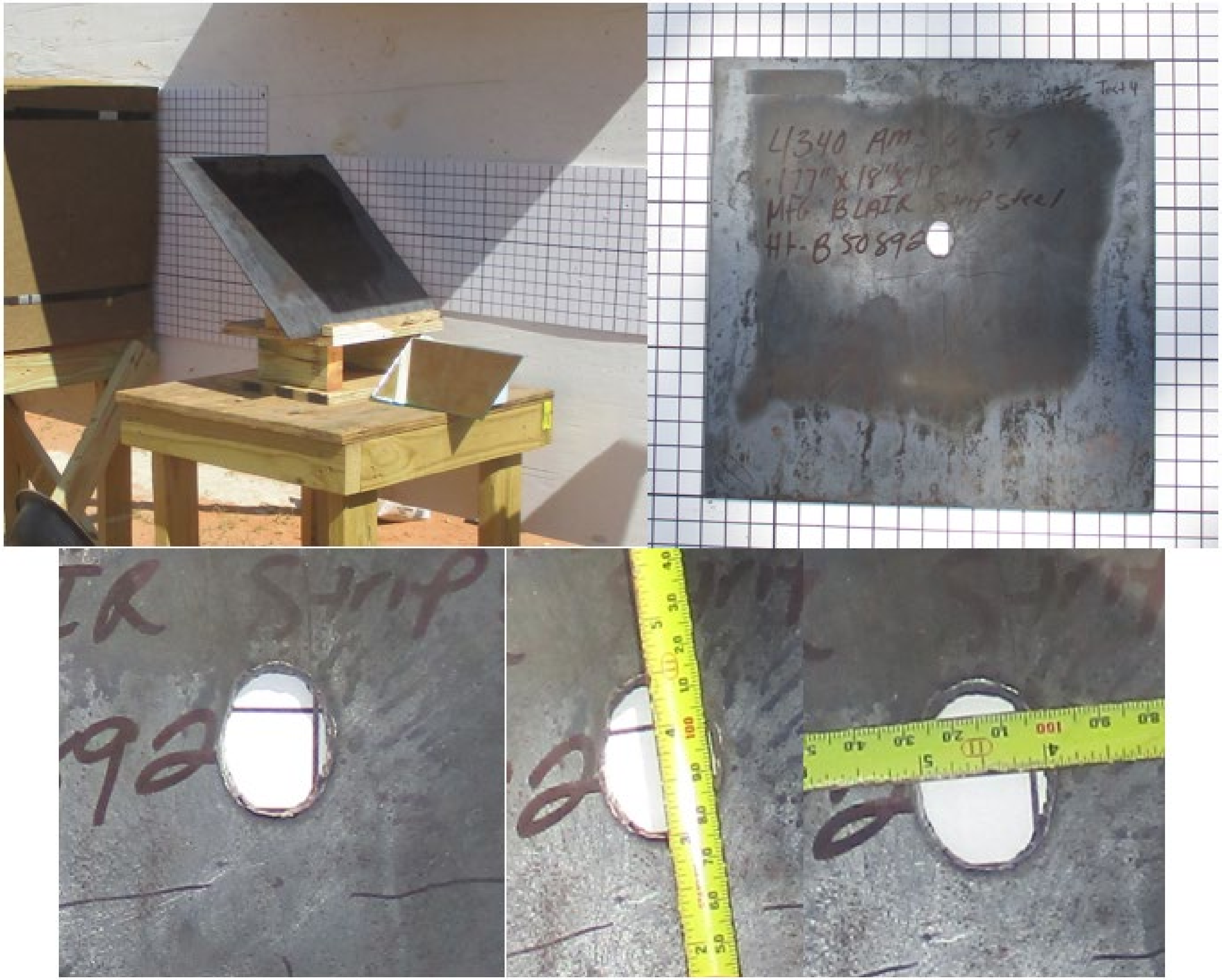

Fig. D4. RT21-472: 4340 RC38 Steel 0.177” Thick, 45 Degrees Obliquity

RT473, 0.125", D2 RC60, 0 DEG OBLIQUITY

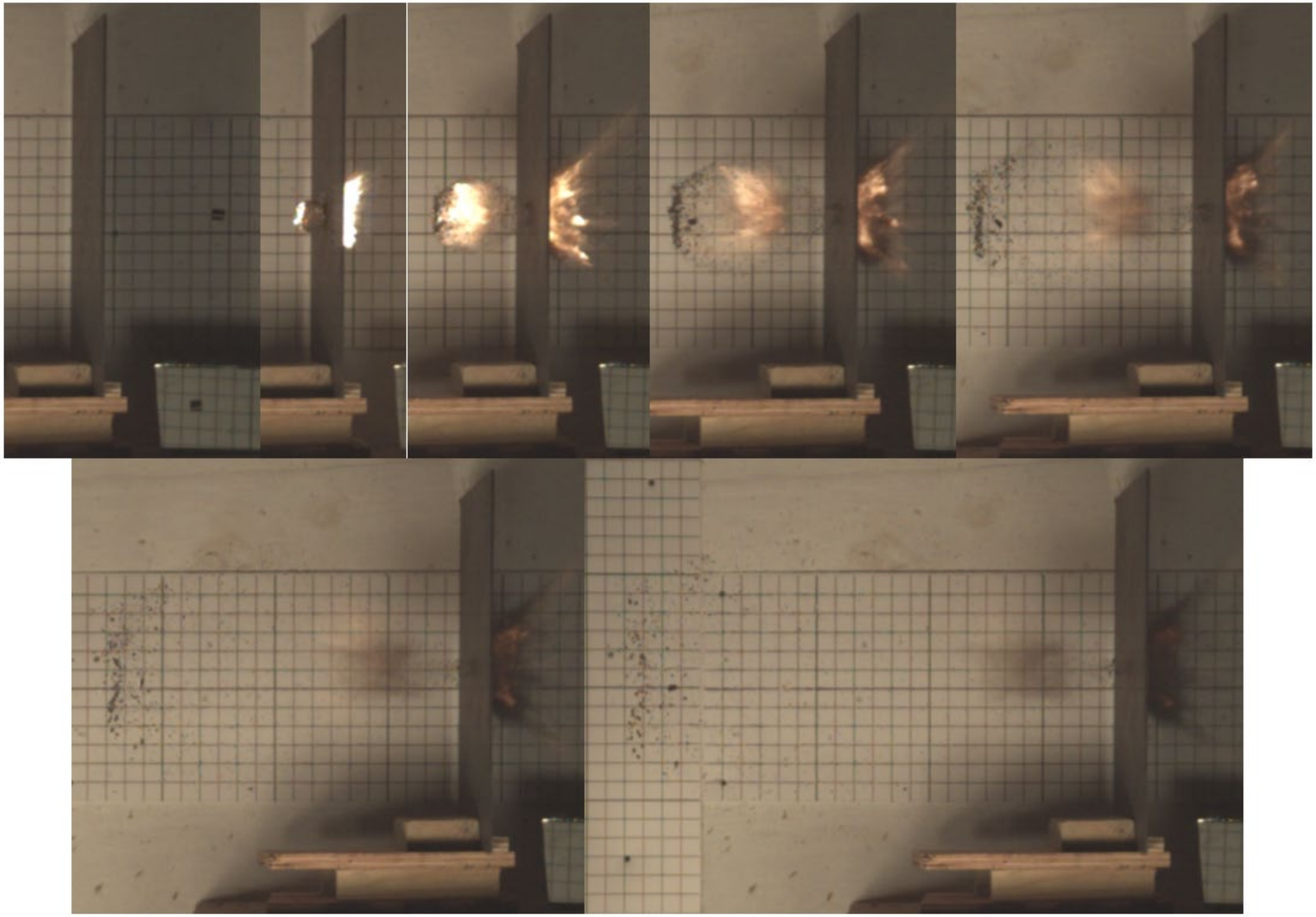

Fig. C5. RT21-473 (0.125", D2 Tool Steel, 0° Obliquity) high speed video frames at -80us, 0us, 40us, 80us, 120us, 240us, 320us

RT473, 0.125”, D2 RC60, 0 DEG OBLIQUITY

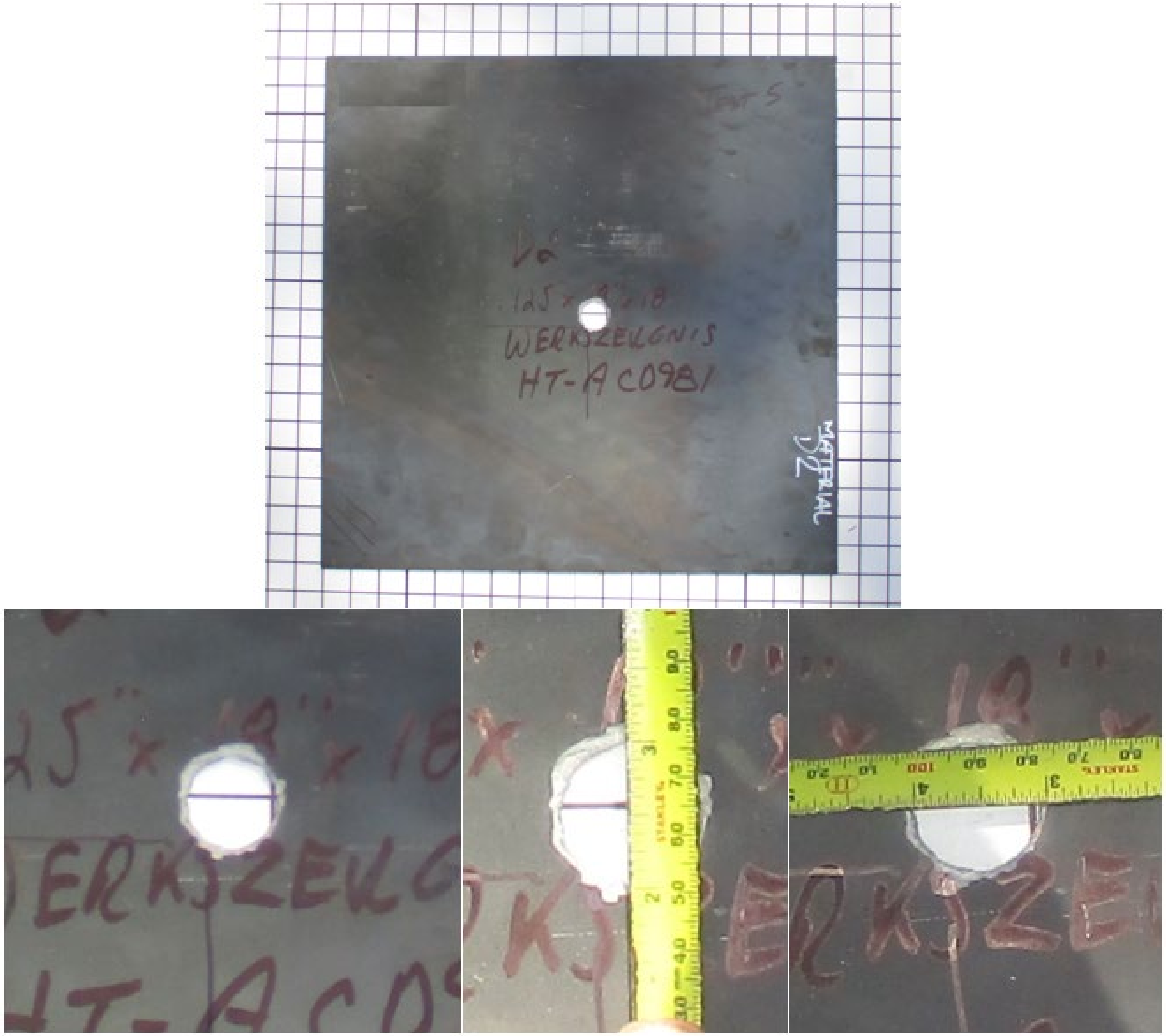

Fig. D5. RT21-473: D2 Tool Steel RC60 0.125” Thick, 0 Degrees Obliquity

RT474, 0.250", D2 RC60, 0 DEG OBLIQUITY

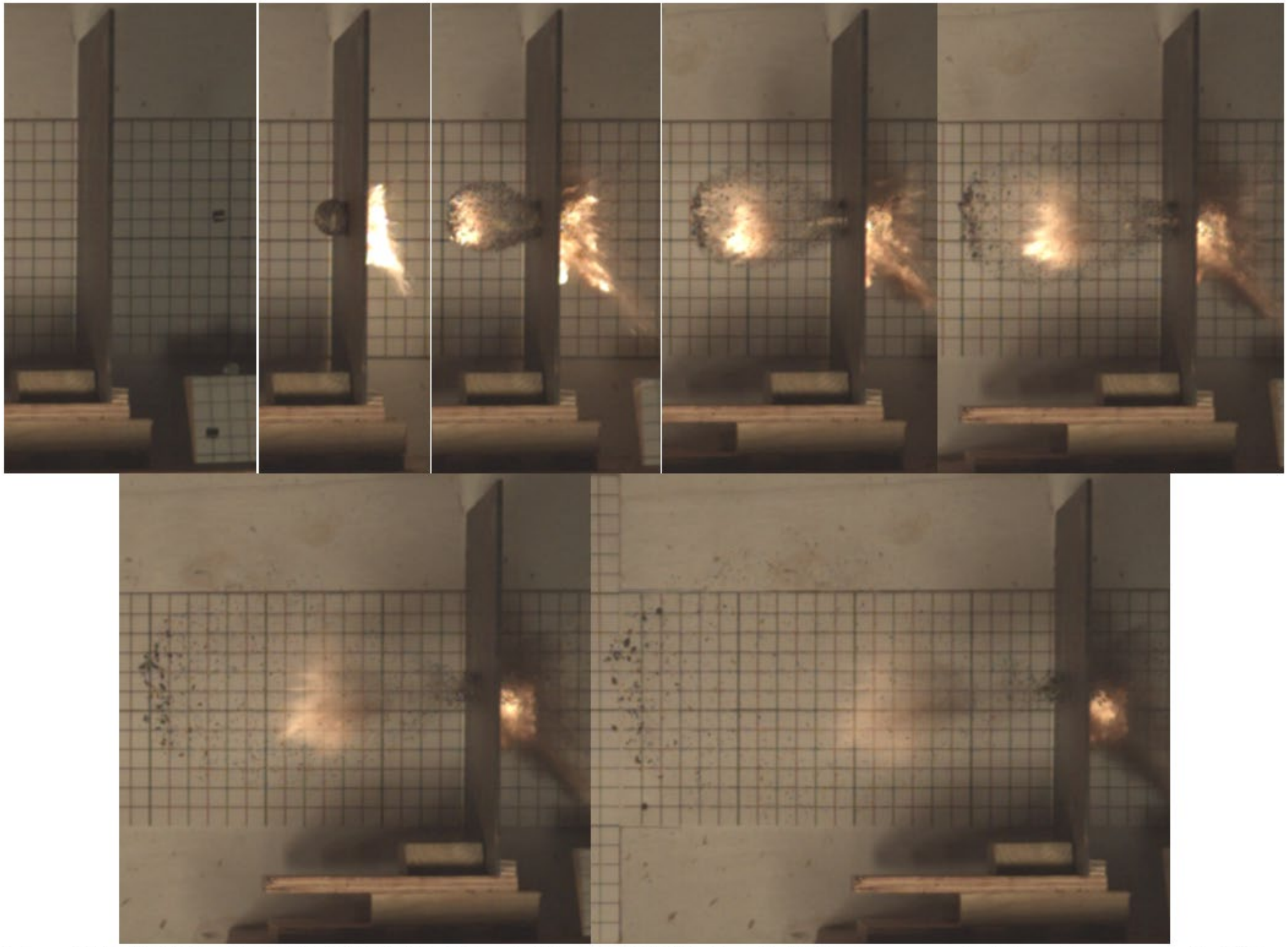

Fig. C6. RT21-474 (0.250", D2 Tool Steel, 0° Obliquity) high speed video frames at -80us, 0us, 40us, 80us, 120us, 240us, 320us

RT474, 0.250", D2 RC60, 0 DEG OBLIQUITY

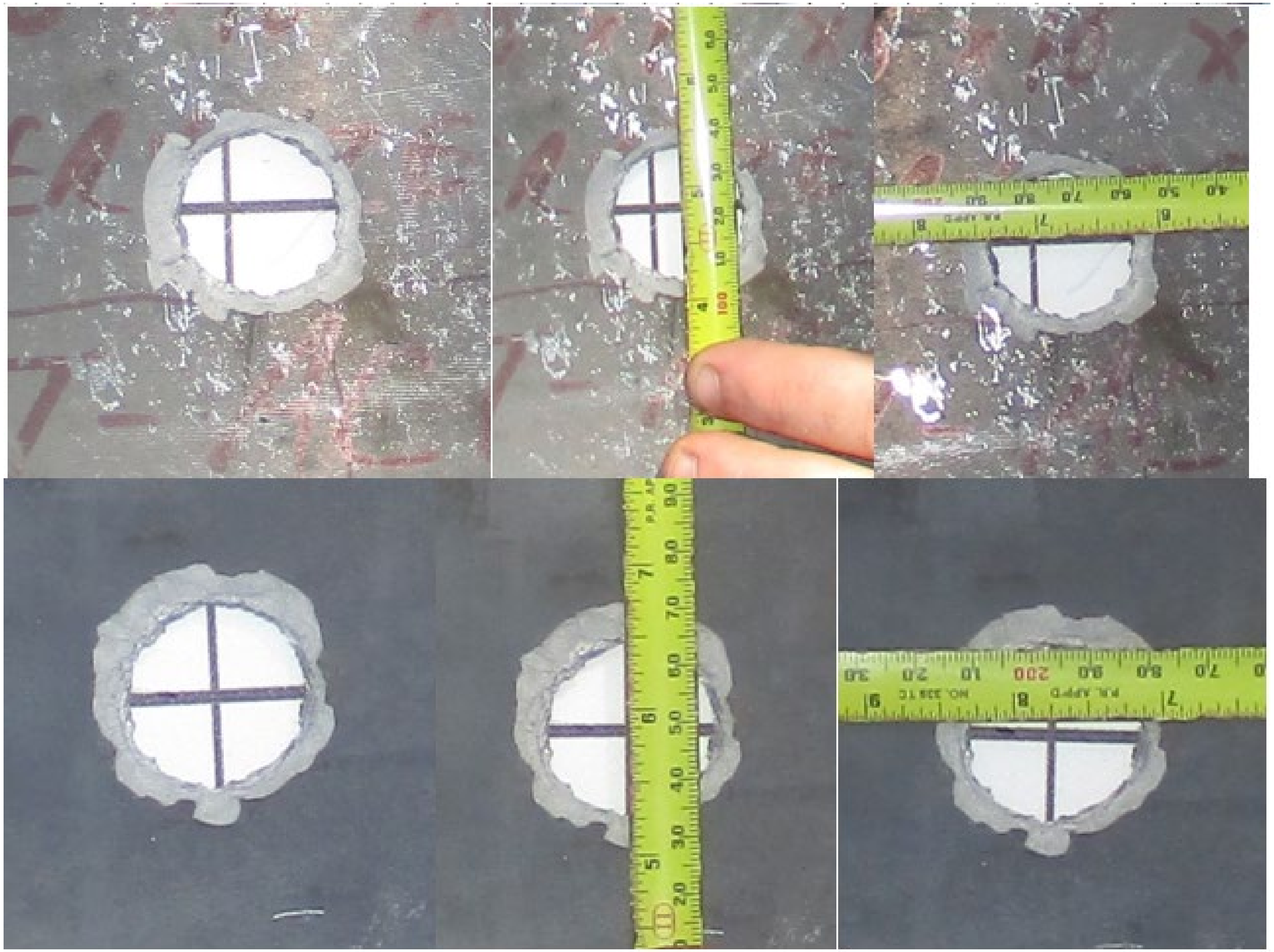

Fig. D6. RT21-474: D2 Tool Steel RC60 0.25" Thick, 0 Degrees Obliquity

RT475, 0.088", D2 RC60, 45 DEG OBLIQUITY

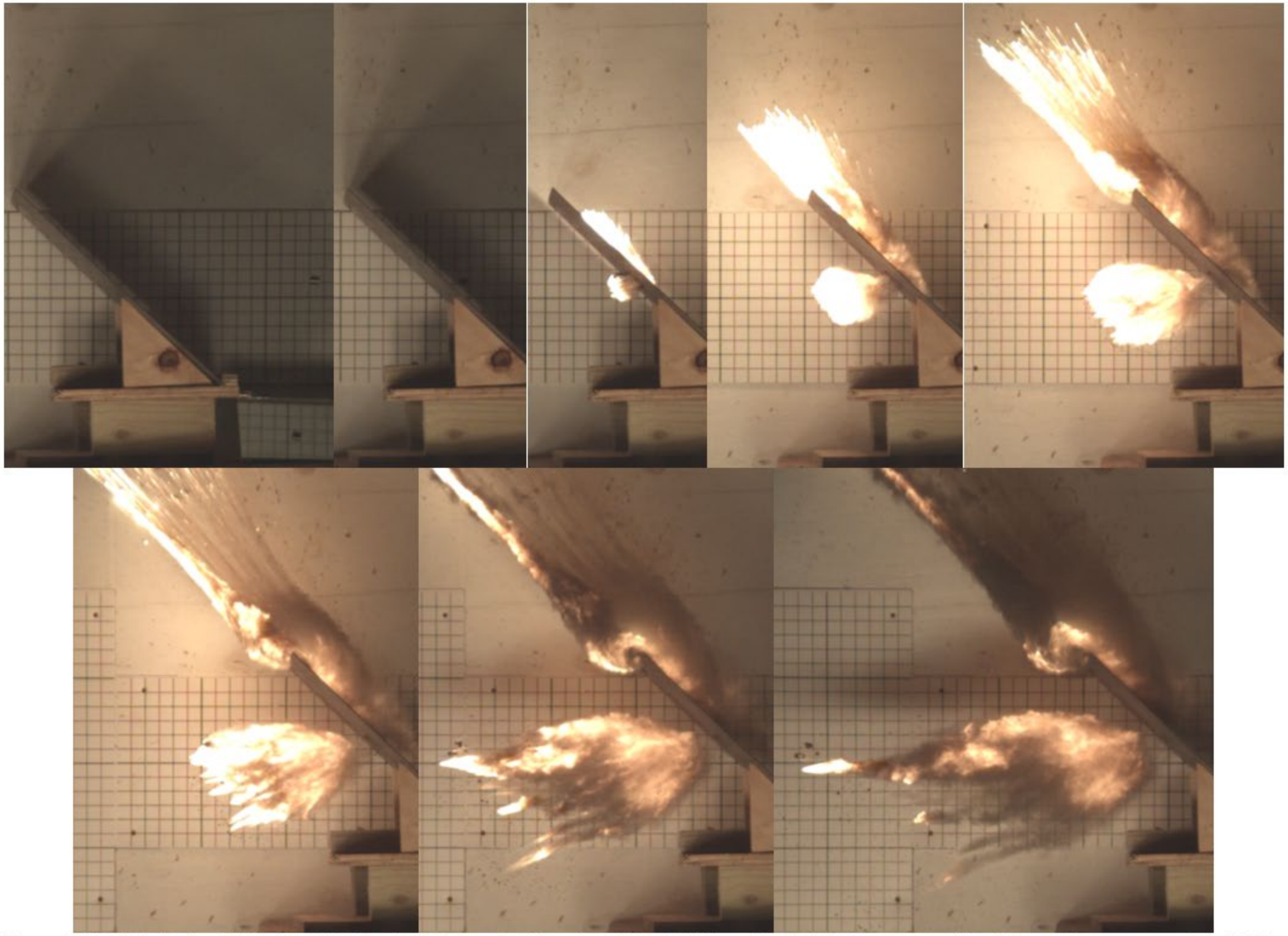

Fig. C7. RT21-475 (0.088", D2 Tool Steel, 45° Obliquity) high speed video frames at -120us, 0us, 40us, 80us, 120us, 240us, 320us

RT475, 0.088”, D2 RC60, 45 DEG OBLIQUITY

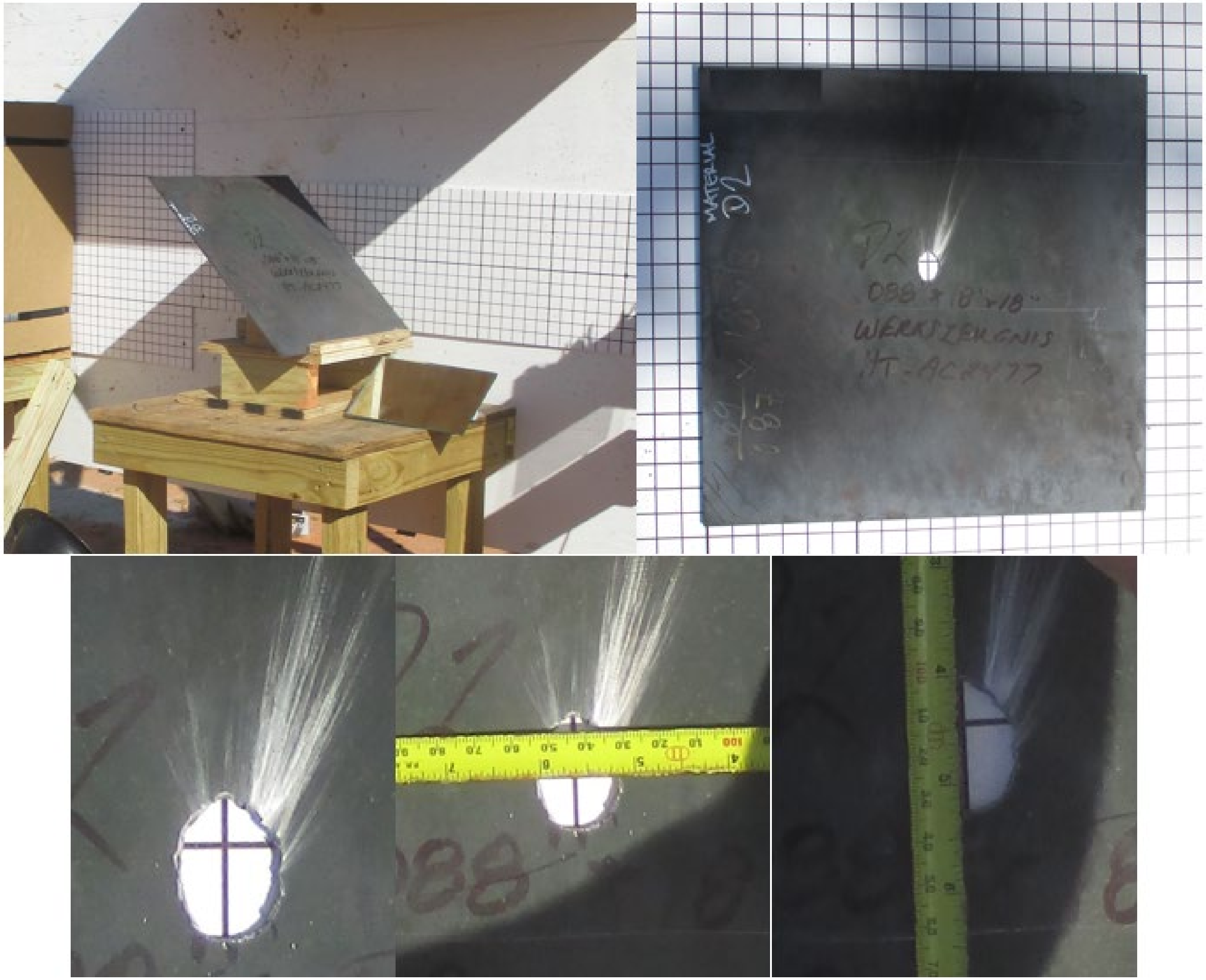

Fig. D7. RT21-475: D2 Tool Steel RC60 0.088” Thick, 45 Degrees Obliquity

RT478, 0.088”, D2 RC60, 45 DEG OBLIQUITY

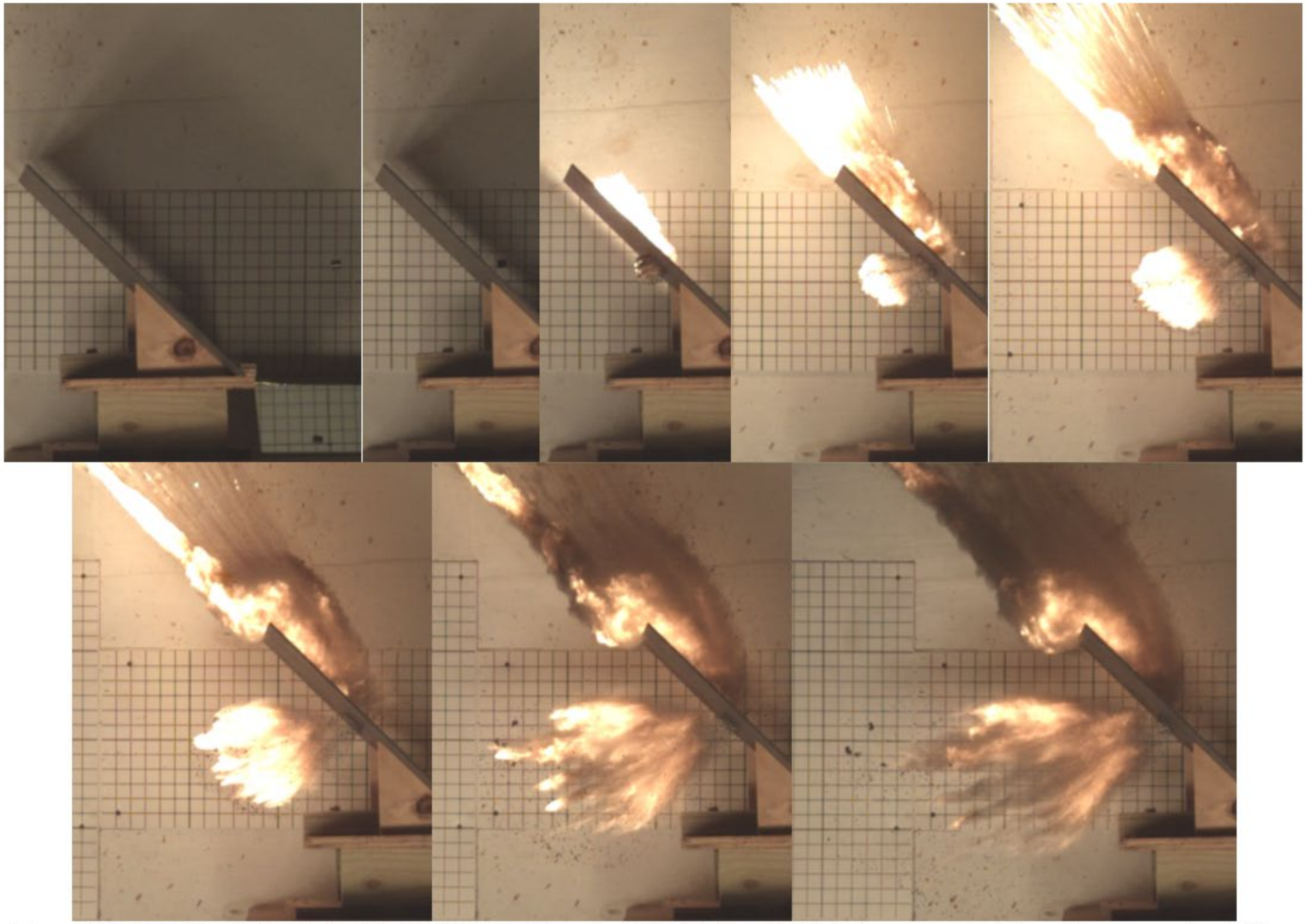

Fig. C8. RT21-478 (0.177”, D2 Tool Steel, 45° Obliquity) high speed video frames at -120us, 0us, 40us, 80us, 120us, 160us, 240us, 320us

RT478, 0.088”, D2 RC60, 45 DEG OBLIQUITY

Fig. D8. RT21-478: D2 Tool Steel RC60 0.177” Thick, 45 Degrees Obliquity

TEST RESULTS – THIN STEEL BARRIERS

DEVCOM ARMAMENTS CENTER

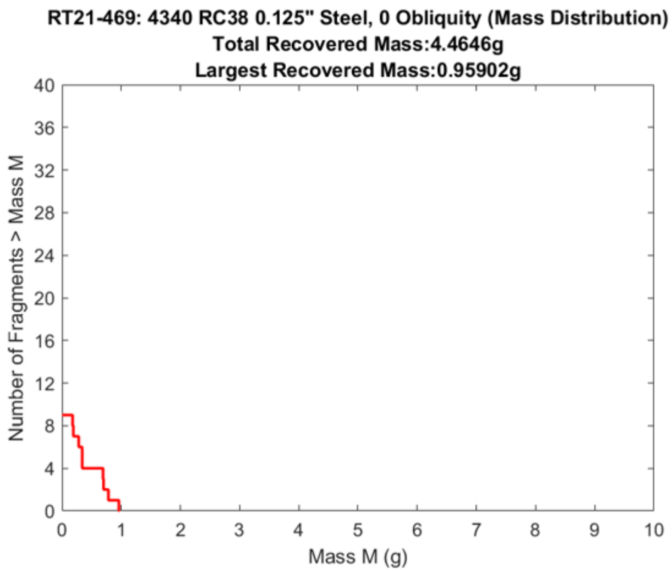

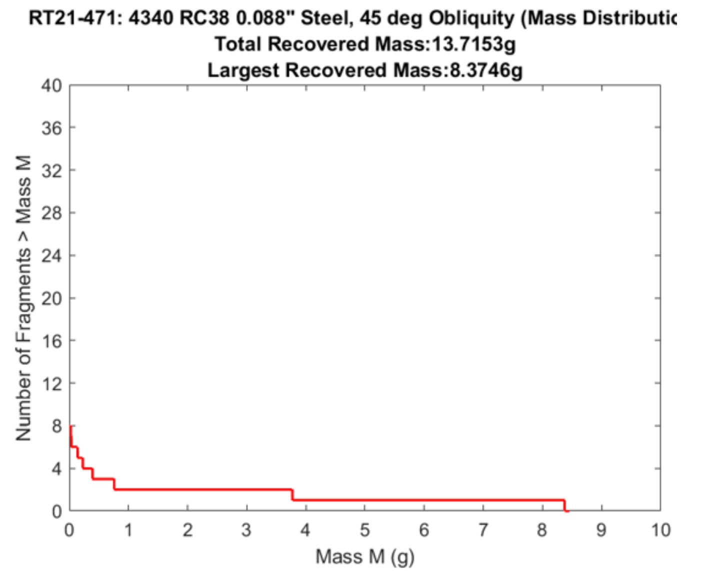

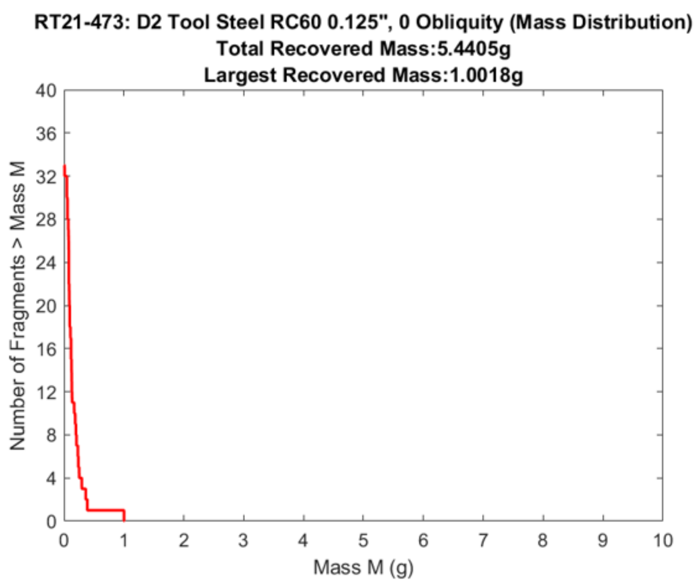

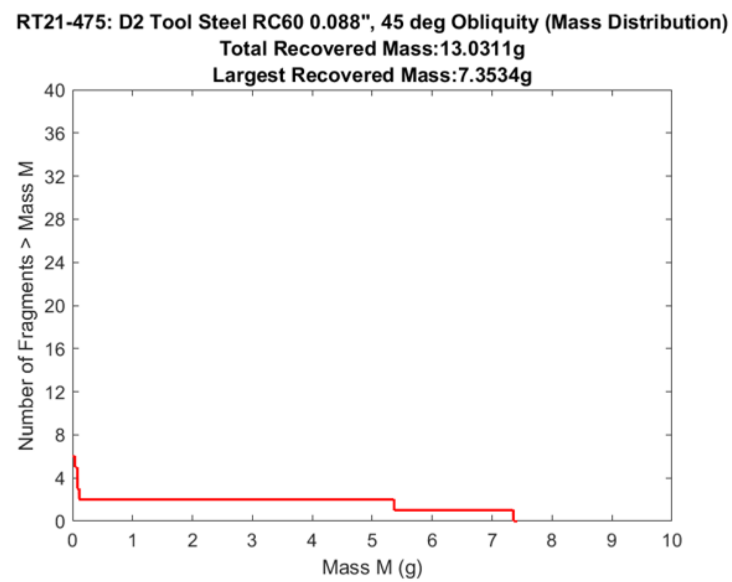

TEST RESULTS – THICK STEEL BARRIERS

RT21-470: 4340 RC38 0.25" Steel, 0 Obliquity (Mass Distribution)
Total Recovered Mass:10.6192g
Largest Recovered Mass:1.2934g

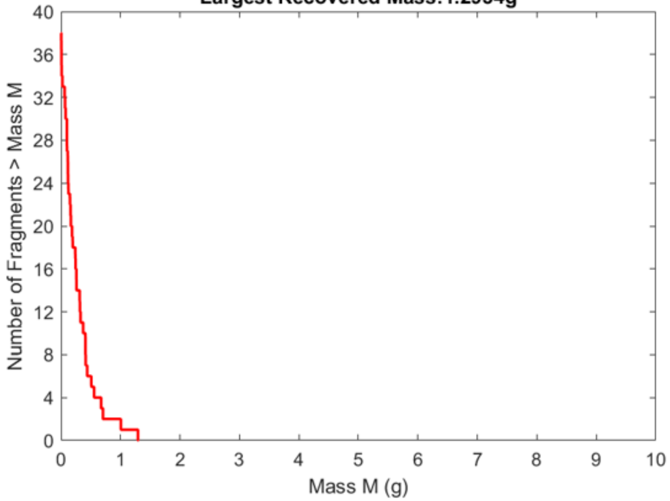

RT21-472: 4340 RC38 0.177" Steel, 45 deg Obliquity (Mass Distribution)
Total Recovered Mass:10.1657g
Largest Recovered Mass:3.4849g

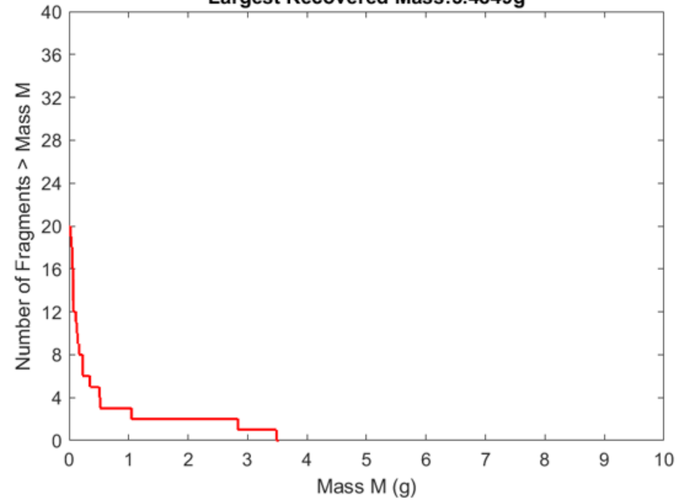

RT21-474: D2 Tool Steel RC60 0.25", 0 Obliquity (Mass Distribution)
Total Recovered Mass:6.2259g
Largest Recovered Mass:0.78147g

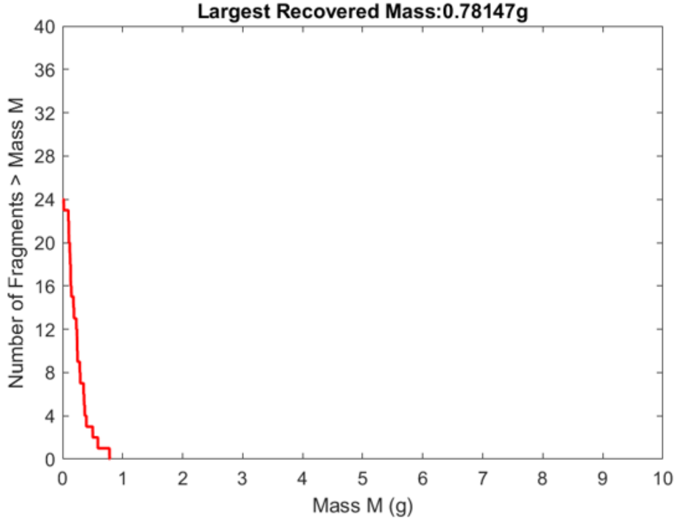

RT21-478: D2 Tool Steel RC60 0.177", 45 deg Obliquity (Mass Distribution)
Total Recovered Mass:10.5946g
Largest Recovered Mass:4.2223g

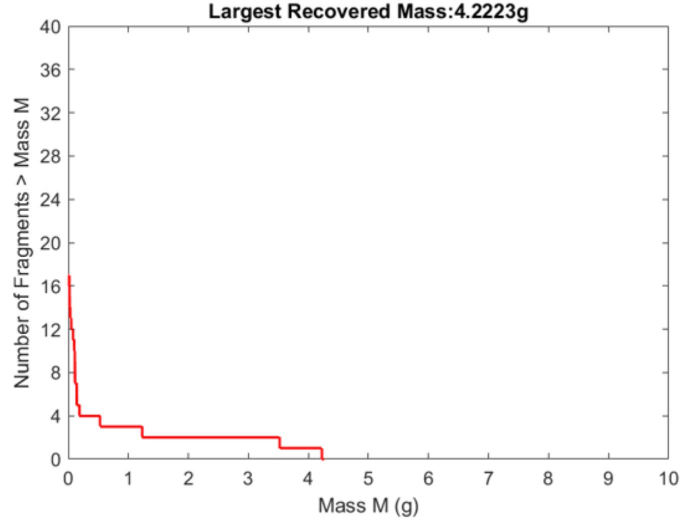

TEST RESULTS

Table 4: Test Results

Test No.	Mat.	Thick. (in)	Obl. (deg)	AD (lb/ft^2)	$V_{S,HSV}$ (ft/s)	$V_{S,TOA}$ (ft/s)	$V_{R,HSV}$ (ft/s)*	ΔV_{HSV} (ft/s)*	$\Delta V_{HSV}/AD$ (ft/s)/(lb/ft^2)*	Total Debris Mass (g)	Largest Frag Mass (g)
469	4340 RC38	0.125	0	5.105	8198	8186	6683	1515	296.8	4.465	0.959
473	D2 RC60	0.125	0	5.105	8475	8383	6842	1633	319.9	5.441	1.002
471	4340 RC38	0.088	45	5.105	8383	8482	6566 6693	1817 1690	355.9 331.1	13.715	8.375
475	D2 RC60	0.088	45	5.105	8489	8456	7146 6728	1343 1761	263.1 345.0	13.031	7.353
470	4340 RC38	0.250	0	10.21	8597	8461	5874	2723	266.7	10.619	1.293
474	D2 RC60	0.250	0	10.21	8539	8400	5857	2682	280.3	6.226	0.782
472	4340 RC38	0.177	45	10.21	8480	8392	5314 5303	3166 3177	310.1 311.2	10.166	3.475
478	D2 RC60	0.177	45	10.21	8297	8383	5986 5623	2311 2674	226.4 261.9	10.595	4.222

*For oblique impacts, top number is front of debris cloud at early times, bottom number is largest debris fragment at late times

TEST RESULTS (CONT'D)

- For all presented areal densities considered, hardness:
  - mildly improves residual velocity at 0 obliquity
  - moderately worsens residual velocity at 45° obliquity
- For the more soft, ductile 4340 RC38 steel
  - Obliquity significantly improved residual velocity
  - Obliquity significantly worsened residual mass
- For the more hard, brittle D2 RC60 steel
  - Obliquity moderately worsened residual velocity
  - Obliquity significantly worsened residual mass

Better residual velocity at obliquity requires good ductility
Fragment breakup highly spall dominated!

PRELIMINARY MODELING

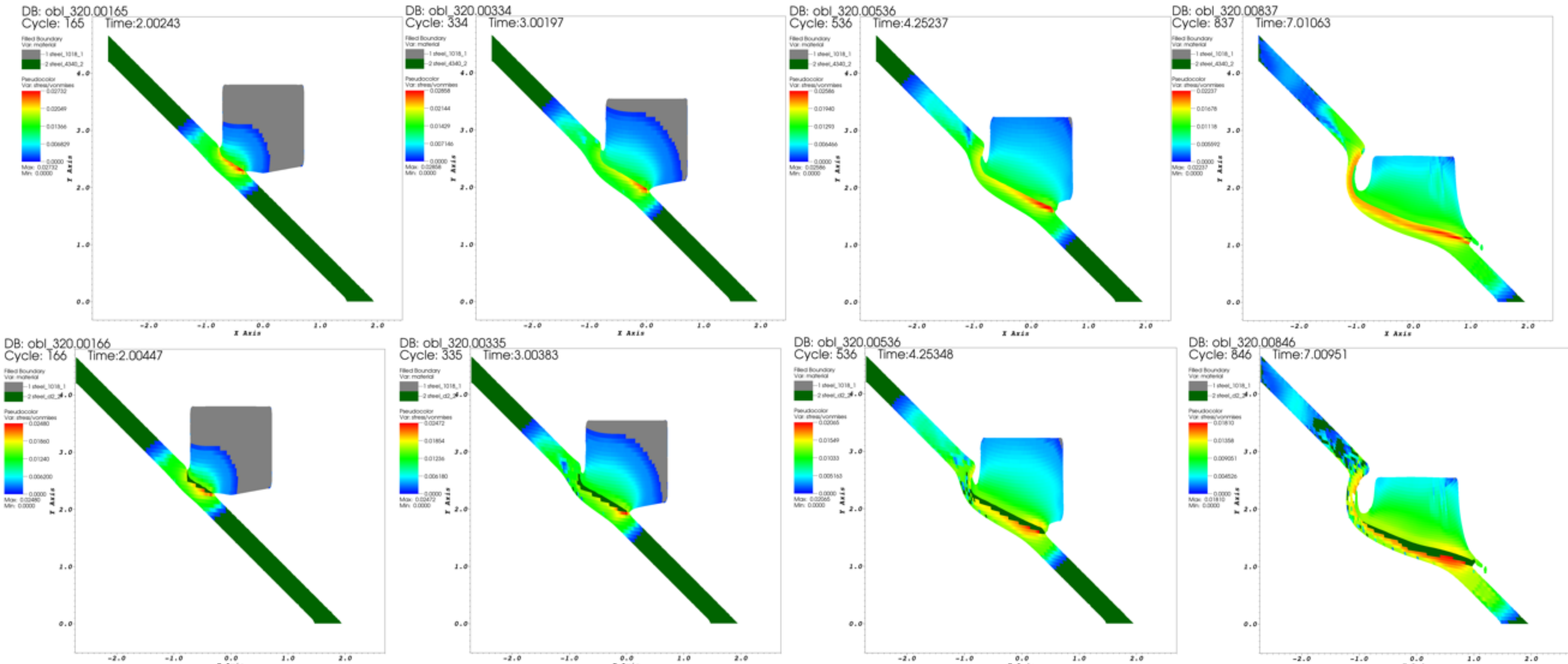

Fig. 5. ALE3D Models to interrogate target failure behavior: 30 kbar spall stress and no failure strain (top row), 10 kbar target spall stress and 0.5 equivalent plastic strain to failure (bottom row)

Obliquity effect does not appear to be caused by spallation ahead of fragment penetration

QUESTIONS

REFERENCES (1 OF 2)

[1] Fragment Impact Test Procedures for Munitions, AOP 4496 Edition A, Version 1, NATO Standardization Office, Brussels, Belgium, March 2019.
[2] Baker, E. L., Al-Shehab, N., Miers, K. T., Pudlak, D. J. "Insensitive Munitions Fragment Impact Gun Testing Technology Challenges". Propellants, Explosives, Pyrotechnics **41**, 572-579 (2016).
[3] Verhoeven, J. D. *Steel Metallurgy for the Non-Metallurgist*. ASM International, 2007.
[4] Hazell, P. J. *Armour: Materials, Theory, and Design*. CRC Press, 2015.
[5] MIL-DTL-32332A, Detail Specification: Armor Plate, Steel, Wrought, Ultra High Hardness. 28 November 2019.
[6] Walker, J. D. *Modern Impact and Penetration Mechanics*. Cambridge University Press, 2021.
[7] Cimpoeru, S. J. "The Mechanical Metallurgy of Armor Steels". DST-Group-TR-3305, Australian Defence Science and Technology Group, October 2016.
[8] Laible, R., Editor. *Ballistic Materials and Penetration Mechanics*. Elsevier, 1980.
[9] Walters, W. P., Zukas, J. A. *Fundamentals of Shaped Charges*. Wiley, 1989.
[10] Grady, D. E. "The spall strength of condensed matter". Journal of the Mechanics and Physics of Solids **36**, 353-384 (1988).
[11] Johnson, G. R., Holmquist, T. J. "Test Data and Computational Strength and Fracture Model Constants for 23 Materials Subjected to Large Strains, High Strain Rates, and High Temperatures". LA-11463-MS, Los Alamos National Laboratory, January 1989.

REFERENCES (2 OF 2)

[12] Mott, N. F. "Fragmentation of Shell Cases". Proc. Royal Society, Vol. 189, Issue 1018, May 1947.

[13] Prifti, J. Catro, M., Squillacioti, R., Cellitti, R. "Improved Rolled Homogeneous Armor (IRHA) Steel Through Higher Hardness". ARL-TR-1347, U.S. Army Research Laboratory, Aberdeen, MD, April 1997.

[14] Showalter, D. D., Gooch, W. A., Burkins, M. S., Koch, R. S. "Ballistic Testing of SSAB Ultra-High-Hardness Steel for Armor Applications". ARL-TR-4632, U.S. Army Research Laboratory, Aberdeen, MD, October 2008.

[15] Gooch, W. A. "Ballistic Testing of French ArcelorMittal Industeel MARS Armor Steels". 14th International Nordmetall Colloquium, Chemnitz, GE, December 2019.

[16] Peterson, N. R., Sweitzer, J. C. "Composite Material Particle Impact Mitigation Sleeve Testing". Procedia Engineering **103** (2015) 475-481.

[17] Peterson, N. R., Al-Shehab, N. M., Sweitzer, J. C., Miller, J. F., Wortman, C. A. "High-Velocity Impact Fragmentation of Projectiles Experimental Results". AMRDEC Technical Report RDMR-WD-16-47 (2016).

[18] Pudlak, D. J. "Development & Demonstration of a Lightweight Particle Impact Mitigation Sleeve (PIMS) with Specified Hardness and Perforation Features". 2018 Insensitive Munitions and Energetic Materials Technology Symposium, Portland, OR, USA, April 2018.

[19] Pudlak, D. J., Al-Shehab, N. M., Miers, K. T., Daniels, A. S., Chang, D. M., Baker, E. L. "Fragment Breakup Investigation Analysis of X-Ray and Computed Tomography Data". 29th JANNAF Propulsion Systems Hazards Joint Subcommittee Meeting, May 2016.

[20] Pudlak, D. J. "Characterization of Fragment Break-up as a Result of Ballistic Impact with Munitions and Associated Materiel". 2016 Insensitive Munitions and Energetic Materials Technology Symposium, Nashville, TN, USA, September 2016.

[21] Murphy, C. H. "Free Flight Motion of Symmetric Missiles". BRL-R-1216, U.S. Army Ballistic Research Laboratory, Aberdeen, MD, July 1963.

[22] Miers, K. T. "High pressure oblique shock interactions in NATO fragment impacts". AIP Conference Proceedings 2272, 120016 (2020).

[23] A. L. Nichols III, Editor, "ALE3D user's manual," LLNL-SM-681737, Lawrence Livermore National Laboratory (2015).